JOURNAL OF Applied Polymer SCIENCE

The Effect of Twin Screw Extrusion on Structural, Electrical, and Rheological Properties in Carbon Nanotube Poly-Ether-Ether-Ketone Nanocomposites

Matthieu Guehenec,[1] Victoria Tishkova,[2] Sylvie Dagreou,[1] Frederic Leonardi,[1] Christophe Derail,[1] Pascal Puech,[2] François Pons,[3] Benedicte Gauthier,[3] Pierre-Henri Cadaux,[3] Wolfgang Bacsa[2]

[1]Université de Pau et des Pays de l'Adour, IPREM, Equipe de Physique et Chimie des Polymères-UMR CNRS/UPPA 5254, Technopole Helioparc, 2, av. Pdt Angot, 64053 Pau Cedex 9, France

[2]CEMES/CNRS, 29 Jeanne Marvig, Université de Toulouse, 31055 Toulouse, France

[3]AIRBUS FRANCE (B.E. M&P Toulouse), 316 Route de Bayonne, 31060 Toulouse, France

Correspondence to: S. Dagreou (E-mail: sylvie.dagreou@univ-pau.fr)

ABSTRACT: The influence of twin screw extruder dispersion of multiwalled carbon nanotubes (CNTs) on the structural, electrical, and rheological properties in poly(ether ether ketone) is studied. Intermediate rotational speeds (200 rpm) of co-rotating twin screws yield higher electrical conductivity and dynamic shear modulus than for lower or higher speeds when using 3 wt % multiwall CNTs. These improved properties at intermediate speeds are correlated with the dispersion state of nanotubes in the polymer matrix by using transmission electron microscopy and multispectral Raman mapping. We find that the complex shear modulus near structural percolation depends on the dispersion of the CNTs and the residence time in the extruder plays an important role in the final properties of the nanocomposite. © 2013 Wiley Periodicals, Inc. J. Appl. Polym. Sci. 129: 2527–2535, 2013

KEYWORDS: composites; nanotubes; rheology; spectroscopy

Received 24 September 2012; accepted 21 December 2012; published online 30 January 2013
DOI: 10.1002/app.38964

INTRODUCTION

The thermal, electrical, and mechanical properties of polymers can substantially improved by incorporating carbon nanotubes (CNTs). CNT reinforced polymers are increasingly used in industry[1] to improve mechanical properties or to make them electrically conducting. High performance thermoplastic polymers are particularly interesting in aeronautic industries due to their thermal stability and excellent mechanical properties. To evacuate static charges[2] and to protect aircrafts against lightning,[3] conducting composites are increasingly gaining importance when replacing metals with composites.

The homogeneous distribution of CNTs in a polymer matrix is a major issue to maintain the needed composite properties at low concentrations of CNTs. Strong Van-der-Waals forces between CNTs lead to agglomerates. Agglomerates can act as imperfections reducing mechanical toughness and the amount of nanotubes available for electrical percolation. There are several strategies to disperse nanotubes such as the use of surfactants[4] or *in situ* polymerization of the matrix.[5–7] But, most dispersion methods are not compatible with large scale industrial applications. Although melt mixing is often used in industry to prepare nanocomposites, extrusion mixing is the simplest method to compound nanocomposites in large quantities.

Twin screw extrusion has been used to disperse CNTs into standard matrices such as, polystyrene (PS),[8] polyacid lactic (PLA),[9] poly(caprolactone) (PCL),[10] polypropylene (PP),[11,12] polycarbonate (PC),[13–17] polyamide (PA),[17,18] polyethyelene (PE),[17] PC/PE blends,[19] polyethylene terephtalate,[20] polybuthylene terephtalate (PBT),[17] but also high performance thermoplastics such as polyether ether ketone [poly(ether ether ketone) (PEEK)].[17,21] Most studies show electrical percolation threshold at low CNT concentrations ranging from 0.5 to 2 wt %. Bauhofer and Kovacs[22] observed that melt mixing often results in a higher percolation threshold than solvent mixing which has been attributed to poorer dispersion. High shear rates when using melt mixing, can damage the nanotubes reducing the form factor[17,23,24] and the final electrical and mechanical properties.

The influence of extrusion parameters on the dispersion of melt-mixed CNT/polymer nanocomposites has been studied by

Additional Supporting Information may be found in the online version of this article.

Pötschke et al.[8,9,13–15,17,18,25] and Tambe et al.[12] These authors investigated the influence of process parameters, such as extruder feeding rate, screw speed and screw profile, temperature, and residence time in the extruder, on the overall distribution of the CNTs in several polymer matrices: PC,[13–15,17] PCL,[25] PLA,[9] PA,[17,18] PS,[8] PP,[12] PBT, LDPE, and PEEK.[17] The specific mechanical energy (SME) developed by the extruder has been used to quantify the changes in the extrusion parameters. It was found that increasing the SME by either, increasing the feeding, screw speed, residence time or by modifying the screw profile, results in a better dispersion. It was demonstrated that there is a critical level of SME above which further improvement of dispersion of the CNTs, no longer improves the electrical conductivity of the nanocomposite.[15] That means that at a critical SME, the percolation network is fully developed. It was furthermore found that CNTs agglomerates are dispersed by two mechanisms during melt mixing: rupture of larger agglomerates into smaller ones and degradation of individual tubes at the frontier between the agglomerates and the matrix.[13–15] The first mechanism appears at high mixing energies while the second is dominant at lower energy levels.

Hwang et al. PP/multiwalled CNT (MWCNT) studied nanocomposites by diluting a 15 wt % master batch by melt mixing and varying the screw speed.[26] It was found that the optimum rheological and conductive properties are not obtained at the highest screw speed but at intermediate screw speed. This has been attributed to the degradation of the CNTs at high screw speeds.

We investigate here the influence of the CNT dispersion in PEEK on the properties of the nanocomposite using transmission electron microscopy (TEM) and Raman spectral imaging. PEEK is a semi crystalline polymer with high thermal, chemical, and mechanical performance. PEEK is used in a wide range of industrial applications.[27] Recently Díez-Pascual et al.[21,28] have demonstrated that mechanical properties of PEEK can be improved by incorporating single wall CNTs (SWCNT) at low concentration. The SWNTs where incorporated by using a solvent-based method. It was shown that the addition of polysulfones as compatibilizers helps to obtain a more uniform SWCNT dispersion but decreases to some degree the electrical conductivity.[10] Bangarasumpath et al. investigated the rheological properties of PEEK/MWCNT composites by extruding a 17 wt % masterbatch and by further diluting to obtain nanocomposites with low CNT content.[29] The rheological percolation threshold has been attributed to the formation of a percolating CNT network where the tube/tube interaction dominates over the polymer chain interaction.

Raman spectroscopy is a nondestructive tool widely used in CNTs analysis. It can be used to determine the dispersion state of CNTs in a polymer matrix as well as the interaction of the CNTs with the environment. Recently, it has been shown that the Raman shift in the G band of double wall CNTs can be used as a local indicator to detect the dispersion of DWNTs in a polymer matrix.[30] TEM is in addition useful to analyze the dispersion of the CNTs in composites in the submicrometer range.

For the applications of CNT composites, it is crucial to improve melt processing. The influence of the processing conditions on final properties of composites needs to be better known. We investigate here the influence of the screw speed of a twin screw extruder on the dispersion of multiwall CNTs in PEEK. The tube dispersion is characterized by multispectral Raman mapping and by TEM. The degree of tube dispersion is then correlated with rheological and electrical measurements of the nanocomposites.

EXPERIMENTAL

We used polyether ether ketone (PEEK) grade 2000 supplied by EVONIK DEGUSSA GmbH in fine powder form (Data from Evonik: $M_w \sim 25{,}000$ g mol^{-1}, $T_g = 143$°C, $T_m = 345$°C $d_{25°C} = 1.2$ g cm^{-3}). MWCNTs Graphistrengh® supplied by ARKEMA (density 50–150 kg m^{-3}, 5–15 layers, average diameter: 15 nm, length: 0.1–10 μm, carbon purity: 90%) were used without further purification.

The PEEK powder was first dried in an oven at 140°C during 6 h to remove moisture. The PEEK powder was then mixed with 3 wt % MWCNTs to form a homogeneous mixture. This mixture was placed into the volumetric hopper feeder specifically designed to contain aerosols. The extruder is set up with a hermetic connection with the hopper feeder observing the national security standards (Institut National de Recherche et de Sécurité standards).[31] The melt compounding was performed in a corotating twin screw extruder from LABTECH engineering company LTD with a ratio L/D equivalent to 40, a screw diameter of 16 mm with 10 different heating zones and a die diameter of 2 mm. The extruder screw profile is assembled from modular screw elements, including transporting elements, kneading and mixing elements. We worked with a screw design with a high shear screw profile as shown on Figure 1. The maximum temperature was set at 390°C, and we used an asymmetric the temperature profile is shown in Table I.

We extruded 500 g of PEEK with 3 wt % MWCNTs at rotor speeds of 100, 150, 200, 300, and 400 rotations per minute (rpm) with a constant throughput of 1 kg h^{-1}. The material leaving the extruder was cooled down in a temperature regulated water bath and then pelletized. The extruded pellets were dried at 140°C in air. The pellets were molded for the rheological measurements by compression at 380°C to obtain disks with a diameter of 25 mm and a thickness of 2 mm. Samples for TEM, Raman, and electrical measurements where prepared from 3 g of the extruded material in the form of dried pellets. Thin films with a thickness of 150 μm and 10 cm in diameter were prepared using a hot press at 380°C. We preheated the pellets during 3min before we pressed at 40 bars during 2 min. The films were cooled down below the crystallization temperature in 3 min before removing the films from the mold.

For the TEM measurements we used an electron microscope Philips CM30 with an acceleration voltage of 150 kV. The samples were cut in 100-nm thick slices with ultramicrotom equipped with a diamond knife.

Raman measurements were performed on an Xplora (Horiba) spectrometer using the 785 nm excitation wavelength. The Raman Imaging was performed on polished surfaces of the composite. We mapped surface areas of 40 × 40 μm^2, 200 ×

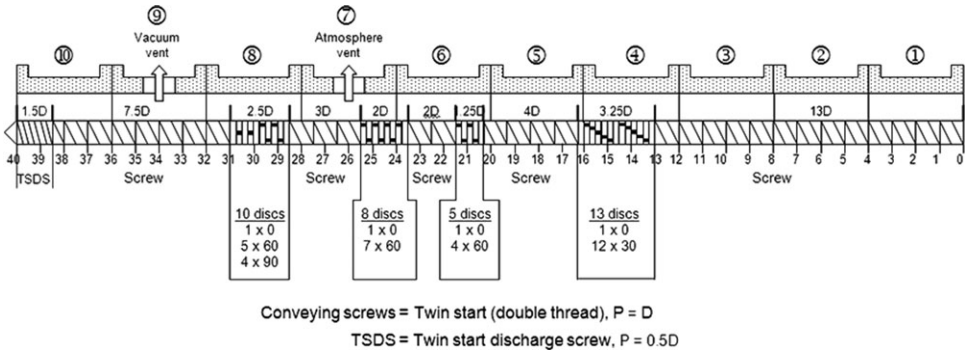

Figure 1. Screw configuration with mixing zone ($L/D = 40 : 1$).

200 μm^2, and 400 × 400 μm^2, in steps of 1.6, 4.4, and 4.6 μm, respectively. Each peak in the spectra was fitted with a Lorentzian line shape and the intensities of the peaks were plotted on the Raman map.

The DC electrical conductivity of PEEK/CNT composites was measured at room temperature using a four wire device connected to a Keithey 6430 electrometer. The films were cut in 3 × 3 cm^2 and cleaned with acetone before testing. The conductivity is given by eq. (1) where V is the voltage applied, t the thickness (cm), and I the current measured.

$$\sigma = \left(\frac{4,532 * v * t}{I}\right)^{-1} \quad (1)$$

Each measurement was performed five times to check for repeatability. The reported values are the mean values. The error is taken as the maximum deviation from the average value.

The rheological measurements were performed on an Advanced Rheometric Expension System (ARES, TA Instrument) using 25-mm diameter parallel plates. All specimens were dried at 140°C before being tested at 360°C under a nitrogen atmosphere to prevent degradation by oxidation. Dynamic strain sweep tests were performed to determine the linear viscoelastic regime. The shear strain amplitude of the experiments was chosen accordingly. We also checked for the stability of the rheological properties by performing time sweep tests. The spectro-mechanical analysis of the samples was determined from 0.1 to 100 rad s^{-1} at a given temperature. We determined all the spectro-mechanical properties at 360°C and all measurements were performed in the linear regime at fixed strain amplitude (0.3%).

The residence time distribution (RTD) consists in recording tracer color concentration against time during the extrusion process. The result shows that the tracer concentration (after passing the dead time t_D) exhibits a maximum before decreasing continuously. The classical RTD with an optic tracer cannot be used here because of the deep black color of the polymer nanotube blend. Instead pellets of PEEK/3 wt % MWCNTs were used as tracer to distinguish from neat PEEK. The residence time is characterized by a fast increase of tracer concentration changing the color from transparent to black. We extruded continuously neat PEEK (grade 2000) before PEEK with 3 wt % of CNTs were manually fed to the hopper. Because of the different viscosity of the neat PEEK and PEEK/MWCNT the real residence time is slightly different. Fang et al.[32] studied the influence of the flow behavior on the RTD. It was concluded that the more viscous the polymer was the longer was the residence time.

The SME is the quantity of energy transmitted to the extruded material per unit of mass. It can be calculated using the eq. (2) where τ is the torque [kJ], N the rotation speed [s^{-1}], and Q_m the throughput [kg s^{-1}].

$$SME = \frac{\tau * N}{Q_m} \quad (2)$$

This energy has been derived by Tara et al.[33] through a study on the flow behavior of starch. The increase of the SME results in an increase of the shear force. The shear force increases with viscosity and screw speed. As a result temperature plays an important role.

RESULTS

To better understand the electrical conductivity and rheological results we use two complimentary methods to study the dispersion of the tubes in the matrix. On the scale of individual tubes, we used TEM to see agglomerates or dispersed tubes. At the micrometer and larger scales we used Raman spectroscopy. Figure 2 shows TEM images obtained for the PEEK/MWCNT composites produced with speed of extrusion 100 rpm (a and c) and 400 rpm (b and d). Figure 2(a,b) show rather good dispersions of MWCNTs. The tubes are entangled and form small agglomerates. On a larger scale [Figure 2(c,d)] one can notice

Table I. Temperature Distribution in Twin Screw Extruder

Zone	Die	9	8	7	6	5	4	3	2	1
Temperature (°C)	370	380	385	390	390	390	385	380	370	360

Applied Polymer SCIENCE

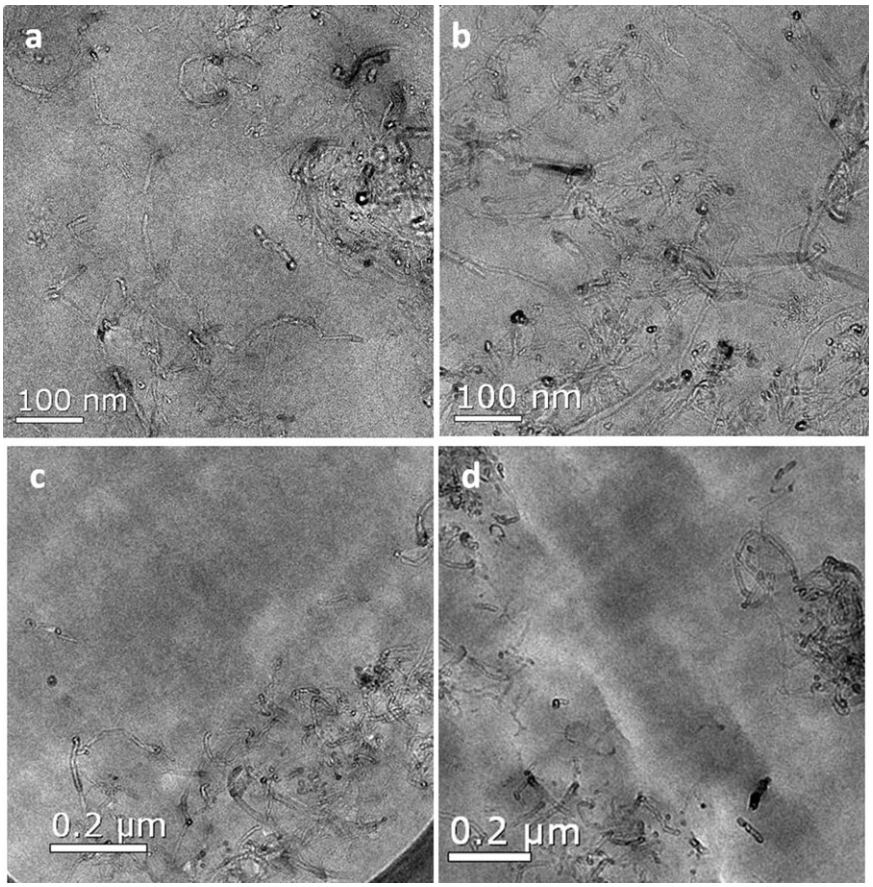

Figure 2. TEM images of PEEK and MWNT composites: rotational speed 100 rpm (a,c), 400 rpm (b and d).

agglomerates of nanotubes and areas with polymer only. All the images show rather good dispersions of the nanotubes.

Figure 3 shows an example of a Raman spectrum obtained for PEEK+MWCNT composite showing the disorder induced D band and G band typical for sp^2 bonded carbon. The peak at 1144 cm^{-1} corresponds to the asymmetric C—O—C stretching vibration in the PEEK polymer.[34] We generated three maps based on the intensities of the D, G bands and the C—O—C band. Figure 4 shows an example of these maps. Black parts correspond to lower intensities while brighter parts to higher intensities. We use the principle of RGB (red, green, bleu) images to present our data. Each map is presented in one of three primary colors (Figure 4); the total image is formed by superimposing the three primary maps. The total image is shown in Figure 4(d). Red and green colors give together yellow. So, the parts which are presented in yellow correspond to the agglomerates of nanotubes. The blue part corresponds to areas with PEEK only. To check for the homogeneity of the tube distribution in the composite, we have recorded maps ranging from 40 to 400 μm. Figure 5 presents the summary of all the data obtained for different scales and different samples. At the lower scales one can notice agglomerates and zones only with polymer for sample prepared at 100 and 400 rpm. At larger scale, 200 by 200 μm, the distribution for all the samples appears homogeneous. And at the largest scale, 400 by 400 μm, one can notice a few big agglomerates, which could not been observed at lower scales.

To quantify the dispersion of the CNTs we calculated the relative noise of the image $2\sigma/\overline{I}$ where σ is the standard deviation and $\overline{I}$ is the mean intensity of the band G over a map.[35] The

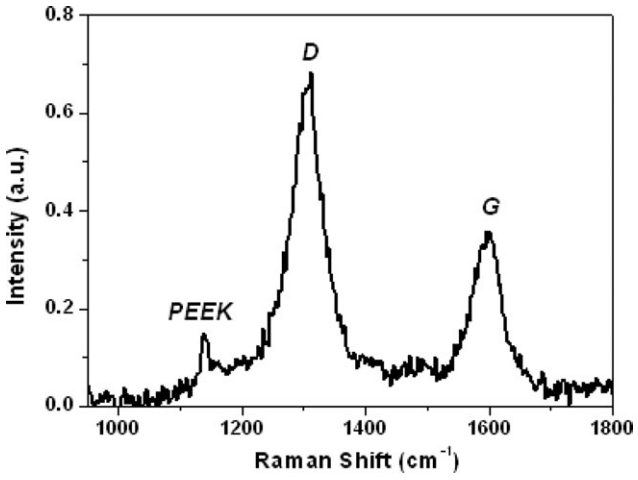

Figure 3. A typical Raman spectrum obtained for a 3 wt % PEEK/MWCNT composite.

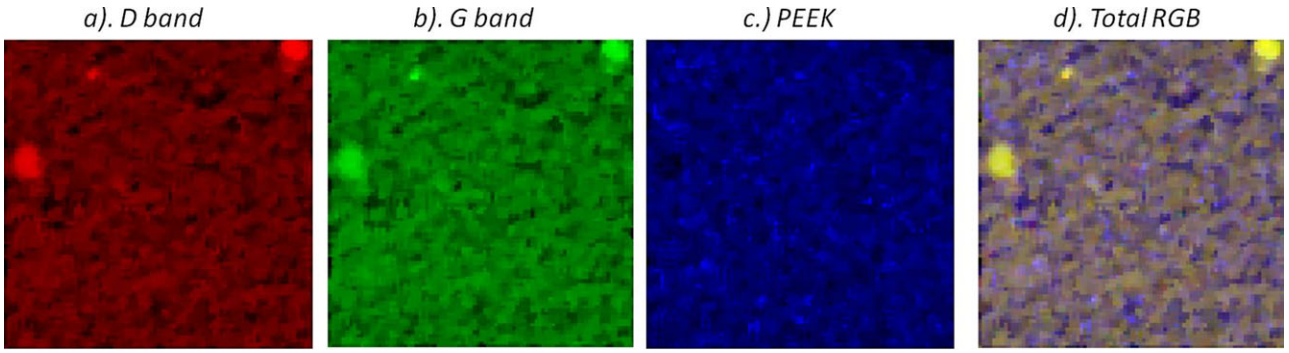

Figure 4. Raman spectral images of the intensities: D band in red (a), G band in green (b) Band from polymer PEEK in blue (c), and superimposed RGB image (d).

minimum of the noise corresponds to best distribution of the MWCNTs. Figure 6 represents the relative noise for all samples and measured at different scales. All the three curves show the same tendency. The minimum of the relative noise falls in the 150–200 rpm range. This means that at medium speed, the dispersion of the CNTs is the more homogeneous compared to fast or slow mixing.

To see whether the tubes are affected by the speed of the twin screw, we calculated the mean Raman spectrum for each area as a function of screw speed and the relative intensity of the D band with respect of the G band was calculated. This relative intensity is often used to characterize the defects in CNTs. Figure 7 shows the results. One can notice that the major tendency is that the relative intensity is decreasing with increasing screw speed. This result is consistent when assuming that shortening of the CNTs at higher screw speed reduces the defects present in the tubes.

Figure 8 shows the dependence of electrical conductivity on screw speed for PEEK/3 wt % MWCNT composite. The inset in Figure 8 shows the electrical conductivity as a function of CNT content when using the highest screw speed (400 rpm). The electrical percolation threshold is found to be at 0.83 wt % of CNTs. This threshold is comparable to that obtained by Socher et al.[17] (0.75 wt %) and Bangarasumpath et al.[29] (1 wt %) for PEEK/MWCNT nanocomposites coumpounded by melt blending. Díez-Pascual obtained a percolation threshold which is much lower (below 0.1 wt %) using SWCNT, which was

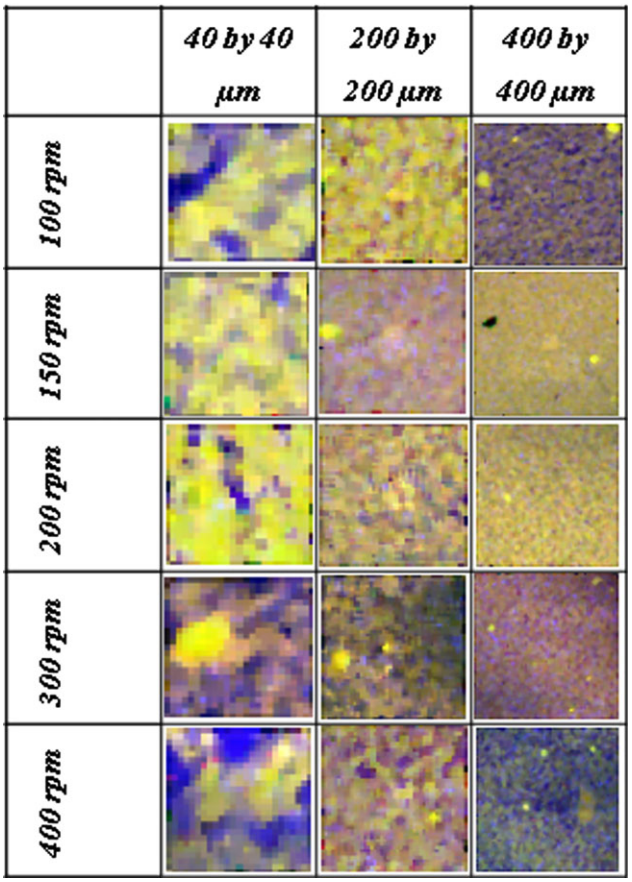

Figure 5. Raman spectral images of the dispersion of MW nanotubes in PEEK matrix presented as RGB images. D band (red), G band (green) give together yellow color, the polymer PEEK is presented in blue.

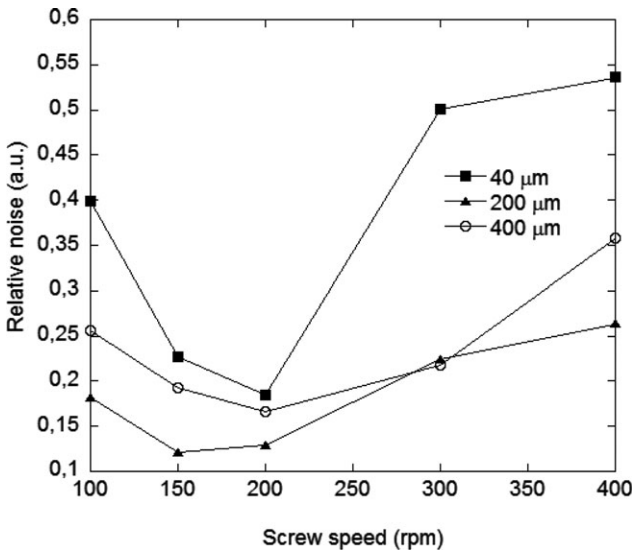

Figure 6. Relative noise $2\sigma/\bar{I}$ for the G band variations in the samples prepared with different speeds. In blue—40 by 40 μm; in red 200 by 200 μm, and in black 400 by 400 μm. The minimum correspond to the best tube dispersion: 150–200 rpm.

Applied Polymer SCIENCE

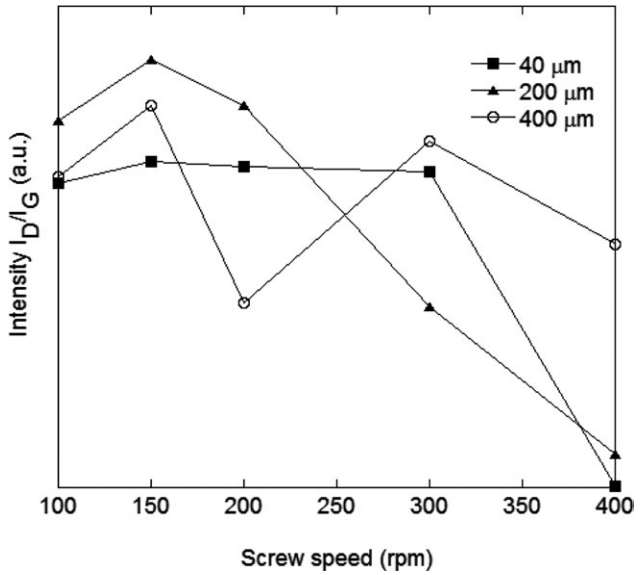

Figure 7. The relative intensity of the D band compared to the G band of the averaged Raman spectra calculated for each investigated area as a function of screw speed.

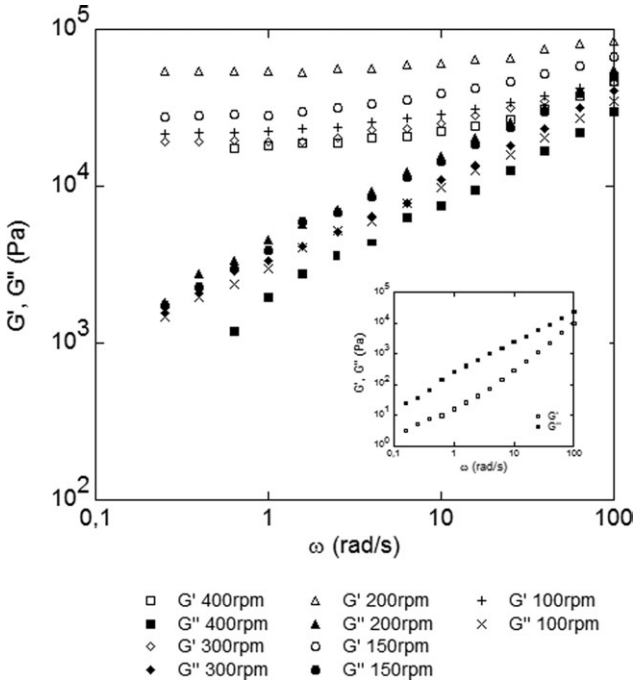

Figure 9. Spectromechanical analysis of PEEK/3 wt %MWCNT prepared with several rotor speeds at 360°C. Feeding rate: 1 Kg h^{-1} and ratio L/D = 40. T = 360°C. Insertion: Spectromechanical analysis of the pure PEEK.

expected because they used solvent-assisted mixing.[28] To investigate the effect of screw speed on the properties of the nanocomposite we have selected a fixed CNT content above the percolation threshold (3 wt %).

In Figure 8, it can be clearly seen that the optimal conductivity is obtained for an intermediate screw speed of 200 rpm. The electrical conductivity rises to 0.05 S cm^{-1} with increasing screw speed until 200 rpm. At higher screw speeds, the electrical conductivity drops off to 0.025 S cm^{-1}. It should be noted that both the optimal conductivity and the best dispersion measured by Raman spectroscopy mapping are obtained for the speed of 200 rpm. For screw speeds lower than 200 rpm, we assume that the shear stress is not high enough to break the nanotubes agglomerates. For higher screw speeds, we observe that the tube dispersion degrades and the electrical conductivity decreases. It should however be mentioned that conductivity drops off at 300 rpm, before slightly increasing at 400 rpm.

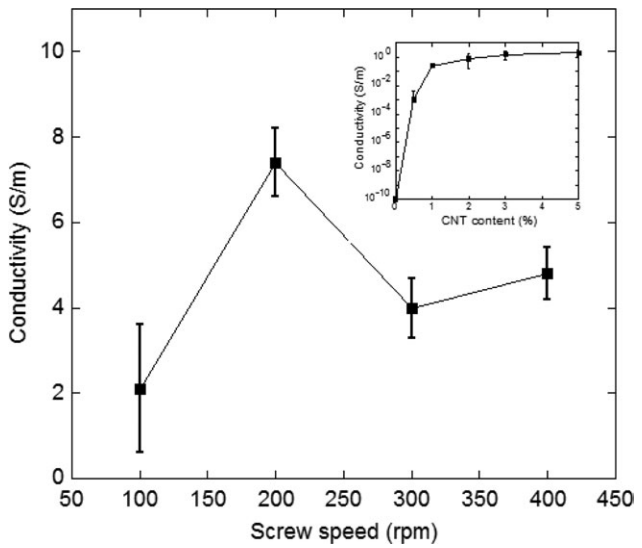

Figure 8. Conductivity σ (S m^{-1}) as a function of screw speed for PEEK/3 wt %MWCNTs. Insertion: Electrical conductivity as a function of CNT content in PEEK at 400 rpm.

Figure 9 shows the mechanical spectra of PEEK with 3 wt % of CNTs extruded at various screw speeds. The insert in this figure shows the spectro-mechanical behavior of the pure PEEK in the same frequency range. The pure PEEK exhibits a liquid-like behavior. The PEEK with 3 wt % MWCNTs show a solid-like behavior with a storage modulus higher than the loss modulus which tends toward a constant value in the low frequency domain. This behavior is typical for polymers filled with particles[36] and for nanocomposites.[28] When the nanoparticle content increases, one observes a liquid to solid transition at low frequency, which is often referred to as the rheological percolation. In our case, the rheological percolation occurs at below 3 wt % of CNTs. A CNT network is formed and prevents the polymer matrix chains to relax.[20,29]

Figure 9 also shows that for all screw speeds, a solid-like behavior at low frequencies is observed. It is found that the complex shear modulus, and specially the storage modulus G′, is very sensitive to the screw speed of the extruder. Both G′ and G″ increase first with increasing screw speed. A maximum is reached when the screw speed is at 200 rpm and the storage modulus doubles when increasing the screw speed from 100 to 200 rpm. When further increasing the screw speed, the values of

the complex shear modules are drastically reduced, reaching values slightly lower than those observed for the lowest speed (100 rpm).

It is interesting to note that rheological properties of nanocomposites are not always sensitive to the dispersion state. For example, in a comprehensive study about the assessment of the dispersion quality of melt-processed clay/poly(ε-caprolactone), Miltner et al.[37] showed that dynamic rheometry was not able to show any difference between samples processed with different residence times, whereas other characterization techniques, such as the measurement of the excess heat capacity, showed clearly differences in the dispersion states. The same insensitivity of the rheological data to the dispersion state was also observed by Mc Clory et al. for PS/MWCNT nanocomposites.[8] We find here that the complex shear modulus is a sensitive parameter for the dispersion state for samples with filler contents closer to the percolation threshold. At the volume fractions studied here, subtle changes in rheological properties can be related to slight modifications of the infinite filler cluster forming throughout the sample. This sensitivity is lost for higher filler rates, where the percolation network is fully developed and the properties are less affected by small changes in the network structure.

DISCUSSION

The Raman spectral mapping at different length scales shows that an optimal dispersion is reached at an intermediate screw speed. The optimum dispersion is well correlated with the optimal conductivity and spectro-mechanical properties. This result is similar to what Hwang et al. have observed[26] but here we show that the improvement of the physical properties correlates with increased tube dispersion. At high speeds, a decrease of the complex viscosity is observed which is attributed to structural changes of MWCNTs at high shear stresses. Our findings are consistent with Pötschke et al.[8,13–15,18] who found that increasing the mixing energy developed during melt blending above a certain critical value will not improve the properties of the obtained nanocomposites, and can affect CNT percolation. So, far it has been thought that nanotubes dispersion improves when increasing the mixing energy, and it has been concluded that, when the percolated network is fully developed, further improvement of dispersion does not improve the obtained properties. But, here we find that increasing the screw speed above the optimum value of 200 rpm results in degradation of the CNT dispersion, and this degradation correlates with the degradation of the physical properties of the nanocomposite.

Recently, several authors have studied the extrusion parameters to evaluate the dependence of the CNT network formation or destruction during the melt mixing process. Pötschke et al.[8] investigated poly lactic acid (PLA) filled with NANOCYL NC7000 CNTs in a master batch and further extrusion processed by co-rotating twin screws with a barrel length of 900 mm ($L/D = 36$) and 1200 mm ($L/D = 48$) at constant throughput of 5 kg h^{-1}. The screw speed was converted into SME to quantify the mechanical energy involved in the mixing process. It was found that higher screw speed and hence higher SME yields better tube dispersion in a PLA matrix. The same conclusions

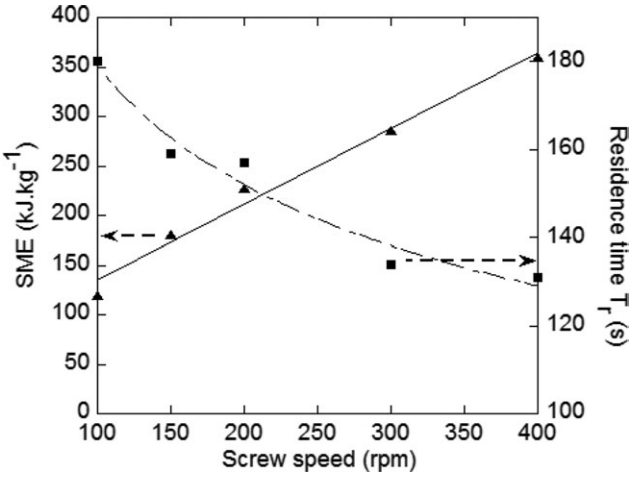

Figure 10. SME (left) and Residence time (right) as a function of screw speed. The line indicates the overall tendency.

were made for poly caprolactone (PCL)/MWCNT composite processed in a similar way.[25] The results were explained by putting forward that a higher SME brings more energy to the mixing process and thus allows better tube dispersion.

It is clear that the screw speed is affecting residence time (t_R). Increasing the screw speed decrease the residence time by 30% in the cases studied by Villmow et al.[25] and Skipa et al.[38] Skipa et al. studied the influence of shear deformation as a function of time on the formation of the CNT network in a PC matrix in the molten state.[38] The network evolution on a PC/MWCNT (from BAYTUBE) nanocomposite was measured by simultaneously monitoring the DC conductivity and the shear modulus for different CNT concentrations and different shear rates showing that the CNT dispersion is related to the shear rate. The electrical conductivity varied considerably when increasing the shear rate. This was attributed to the formation of the CNT network or destruction as the shear rate is increased. It was demonstrated that after a certain shear time, the rheological and electrical measurements reach a steady state. Hwang et al.[26] have also worked on the extrusion processing condition on PP/MWCNT nanocomposites prepared by diluting master batches using NANOCYL NC7000 nanotubes and a extruder with a large L/D ratio. Unlike Villmow et al.,[9] the authors obtained an optimal dispersion at an intermediate screw speed of 200 rpm. The dispersion was characterized by mechanical, rheological and electrical measurements, and using TEM. It was concluded that a high screw speed damages the MWCNTs.

The different studies show that the extrusion process parameters (screw speed, screw profile, barrel length, and flow rate) have an important impact on CNT dispersion. The different process parameters influence two main factors (i) the energy transferred during the process (SME) and (ii) the residence time. These are the two main factors to consider when comparing composites processed under different conditions. Figure 10 shows the SME developed by the extruder during melt mixing, and the residence times. The SME has been determined using the same

method as Villmow et al.[25] In our study, we obtain optimal dispersion and nanocomposite properties, as Hwang et al.[26] at intermediate screw speeds. Unfortunately, we cannot directly compare our extrusion parameters since the SME and residence time is not known for the work of Hwang et al. But, we can compare our processing conditions to the work of Villmow et al.[25] The screw profile is similar but no back conveying elements and ending kneading zones have been used in our process. In addition we note that *L*/*D* ratio, we are using is smaller. The specific mechanical energies developed by our process are similar for the same screw speed, but our residence time is about 30% longer. This indicates that a longer residence time leads to the observed differences. Two hypotheses can be made to explain that poorer dispersions are obtained when increasing the screw speed above 200 rpm. High SME destroys the CNT network at longer residence time or the CNTs are damaged by high SME and longer residence time. Moreover, we observed that electrical conductivity increases again at 400 rpm: to interpret this effect, we can make the hypothesis of a competition between improvement of dispersion at high SME, and breakage of nanotubes.

CONCLUSIONS

We studied the influence of the extruder screw speed on the dispersion of CNT in PEEK. We find that the rheological and electrical properties change in a nonlinear way with screw speed. Both electrical conductivity and shear modulus show an optimum at intermediate screw speed of 200 rpm. Extensive Raman spectral mapping at different scales show that CNTs are better dispersed at intermediate screw speed showing that both the shear modulus and the electrical conductivity are directly influenced by the dispersion state. Degradation of the physical properties at higher screw speeds is associated with destruction of CNT percolation network and shortening of the CNTs.

ACKNOWLEDGMENTS

This work has been carried out in the framework of the InMat project, led by Airbus France (BE M&P Toulouse). The authors thank the DGCIS and the region Midi-Pyrénées for funding the present work.

REFERENCES

1. Dai, L.; Mau, A. W. H. *Adv. Mater.* **2001**, *13*, 12.
2. Markarian, J. *Plast. Addit. Compound.* **2005**, *7*, 26.
3. Li, N.; Huang, Y.; Du, F.; He, X.; Lin, X.; Gao, H.; Ma, Y.; Li, F.; Chen, Y.; Eklund, P. C. *Nano Lett.* **2006**, *6*, 1141.
4. Pang, J.; Xu, G.; Yuan, S.; Tan, Y.; He, F. *Colloids Surf A* **2009**, *350*, 101.
5. Ahir, S. V.; Huang, Y. Y.; Terentjev, E. M. *Polymer* **2008**, *49*, 3841.
6. Courbaron-Gilbert, A.; El-Bounia, N. E.; Péré, E.; Billon, L.; Derail, C. *Adv. Mater. Res.* **2010**, *112*, 29.
7. Datsyuk, V.; Guerret-Piecourt, C.; Dagréou, S.; Billon, L.; Dupin, J.-C.; Flahaut, E.; Peigney, A.; C. Laurent. *Carbon* **2005**, *43*, 873.
8. Mc Clory, C.; Pötschke, P.; Mc Nally, T. *Macromol. Mater. Eng.* **2011**, *296*, 59.
9. Villmow, T.; Pötschke, P.; Pegel, S.; Häussler, L.; Kretzschmar, B. *Polymer* **2008**, *49*, 3500.
10. Díez-Pascual, A. M.; Naffakh, M.; González-Domínguez, J. M.; Ansón, A.; Martínez-Rubi, Y.; Martínez, M. T.; Simard, B.; Gomez, M. A. *Carbon* **2010**, *48*, 3485.
11. Müller, M. T.; Krause, B.; Kretzschmar, B.; Pötschke, P. *Compos. Sci. Technol.* **2011**, *71*, 1535.
12. Tambe, P. B.; Bhattacharyya, A. R.; Kulkarni, A. R. *J. Appl. Polym. Sci.* **2013**, *127*, 1017.
13. Kasaliwal, G.; Göldel, A.; Pötschke, P. *J. Appl. Polym. Sci.* **2009**, *112*, 3494.
14. Kasaliwal, G.; Göldel, A.; Pötschke, P.; Heinrich, G. *Polymer* **2011**, *52*, 1027.
15. Kasaliwal, G.; Pegel, S.; Göldel, A.; Pötschke, P.; Heinrich, G. *Polymer* **2010**, *51*, 2708.
16. Pötschke, P.; Fornes, T. D.; Paul, D. R. *Polymer* **2002**, *43*, 3247.
17. Socher, R.; Krause, B.; Müller, M.; Boldt, R.; Pötschke, P. *Polymer* **2012**, *53*, 495.
18. Krause, B.; Pötschke, P.; Häubler, L. *Compos. Sci. Technol.* **2009**, *69*, 1505.
19. Pötschke, P.; Bhattacharyya, A. R.; Janke, A. *Carbon* **2004**, *42*, 965.
20. Hu, G.; Zhao, C.; Zhang, S.; Yang, M.; Wang, Z. *Polymer* **2006**, *47*, 480.
21. Díez-Pascual, A. M.; Naffakh, M.; Gomez, M. A.; Marco, C.; Ellis, G.; Martínez, M. T.; Ansón, A.; González-Domínguez, J. M.; Martínez-Rubic, Y.; Simard, B. *Carbon* **2009**, *47*, 3079–3090.
22. Bauhofer, W.; Kovacs, J. Z. *Compos. Sci. Technol.* **2009**, *69*, 1486.
23. Xu, D.-H.; Wang, Z.-G. *Macromolecules* **2008**, *41*, 815.
24. Krause, B.; Boldt, P.; Pötschke, P. *Carbon* **2011**, *49*, 1243.
25. Villmow, T.; Kretzschmar, B.; Pötschke, P. *Compos. Sci. Technol.* **2010**, *70*, 2045.
26. Hwang, T. Y.; Kim, H. J.; Ahn, Y. *Korea-Aust. Rheol. J.* **2010**, *22*, 141.
27. Jones, D. P.; Leach, D. C.; Moore, D. R. *Polymer* **1985**, *26*, 1385.
28. Diez-Pascual, A. M.; Naffakh, M.; Gomez, M. A.; Marco, C.; Ellis, G.; Gonzalez-Dominguez, J. M.; Anson, A.; Martinez, M. T.; Martinez-Rubi, Y.; Simard, B.; Ashrafi, B. *Nanotechnology* **2009**, *20*, 315707(315713pp).
29. Bangarusampath, D. S.; Ruckdäschel, H.; Altstädt, V.; Sandler, J. K. W.; Garray, D.; Shaffer, M. S. P. *Polymer* **2009**, *50*, 5803.

30. Tishkova, V.; Raynal, P.-I.; Puech, P.; Lonjon, A.; Fournier, M. L.; Demont, P.; Flahaut, E.; Bacsa, W. A. *Compos. Sci. Technol.* **2011**, *71*, 1326.

31. Institut National de Recherche et de Sécurité, "Nano-matériaux, risques pour la santé et mesures de prévention", 2011, to be consulted at http://www.inrs.fr/accueil/risques/chimiques/focus-agents/nanomateriaux.html, **2011**.

32. Fang, H.; Mighri, F.; Ajji, A.; Cassagnau, P.; Elkoun, S. *J. Appl. Polym. Sci.* **2011**, *120*, 2304.

33. Tara, A.; Berzin, F.; Tighzert, L.; Moughamir, S. *Rhéologie* **2005**, *8*, 5.

34. Stuart, B. H. *Spectrochim. Acta Part A* **1997**, *Part A*, 107.

35. Bellayer, S.; Gilman, J. W.; Eidelman, N.; Bourbigot, S.; Flambard, X.; Fox, D. M.; Long, H. C. D.; Trulove, P. C. *Adv. Funct. Mater.* **2005**, *15*, 910.

36. Inoubli, R.; Dagréou, S.; Lapp, A.; Billon, L.; Peyrelasse, J. *Langmuir* **2006**, *22*, 6683.

37. Miltner, H. E.; Watzeels, N.; Goffin, A.-L.; Duquesne, E.; Benali, S.; Dubois, P.; Rahier, H.; Van Mele, B. *J. Mater. Chem.* **2010**, *20*, 9531.

38. Skipa, T.; Lellinger, D.; Böhm, W.; Saphiannikova, M.; Alig, I. *Polymer* **2010**, *51*, 201.